The EMBO Journal vol.14 no.18 pp.4578–4588, 1995

Protein–rRNA binding features and their structural and functional implications in ribosomes as determined by cross-linking studies

Henning Urlaub, Volker Kruft[1], Oliver Bischof, Eva-Christina Müller and Brigitte Wittmann-Liebold[2]

Max-Delbrück-Centrum für Molekulare Medizin, Robert-Rössle Straße 10, D-13125 Berlin, Germany
[1]Present address: Applied Biosystems GmbH, Brunnenweg 13, D-64331 Weiterstadt, Germany

[2]Corresponding author

We have investigated protein–rRNA cross-links formed in 30S and 50S ribosomal subunits of *Escherichia coli* and *Bacillus stearothermophilus* at the molecular level using UV and 2-iminothiolane as cross-linking agents. We identified amino acids cross-linked to rRNA for 13 ribosomal proteins from these organisms, namely derived from S3, S4, S7, S14, S17, L2, L4, L6, L14, L27, L28, L29 and L36. Several other peptide stretches cross-linked to rRNA have been sequenced in which no direct cross-linked amino acid could be detected. The cross-linked amino acids are positioned within loop domains carrying RNA binding features such as conserved basic and aromatic residues. One of the cross-linked peptides in ribosomal protein S3 shows a common primary sequence motif—the KH motif—directly involved in interaction with rRNA, and the cross-linked amino acid in ribosomal protein L36 lies within the zinc finger-like motif of this protein. The cross-linked amino acids in ribosomal proteins S17 and L6 prove the proposed RNA interacting site derived from three-dimensional models. A comparison of our structural data with mutations in ribosomal proteins that lead to antibiotic resistance, and with those from protein–antibiotic cross-linking experiments, reveals functional implications for ribosomal proteins that interact with rRNA.

Keywords: antibiotics/cross-linked ribosomal proteins/KH-motif/protein–RNA interaction/zinc finger-like motif

Introduction

Ribosomes are highly complex ribonucleoprotein particles responsible for protein synthesis in all living cells. Without detailed knowledge of the molecular structure and topography of ribosomal components, the translational process in which many molecules are involved cannot be understood. Several approaches have led to models of the overall topography of ribosomes, whereas topographical data at the peptide and amino acid level are only available for some cross-linked protein pairs (e.g. S13–S19, Brockmüller and Kamp, 1988; Pohl and Wittmann-Liebold, 1988; L3–L19, Herwig *et al.*, 1993; L23–L29, Bergmann and Wittmann-Liebold, 1993) and for some protein–RNA cross-links (e.g. Ehresmann *et al.*, 1976; Maly *et al.*, 1980), since cross-linked proteins cannot be isolated readily in sufficient amounts. More recently, crystallographic data obtained from several ribosomal proteins such as S5 (Ramakrishnan and White, 1992), S6 (Lindahl *et al.*, 1994), L6 (Golden *et al.*, 1993a), L7/L12 (Leijonmark *et al.*, 1980), L9 (Hoffman *et al.*, 1994) and L30 (Wilson *et al.*, 1986) have allowed more insight to be gained concerning protein–RNA interactions within the ribosome. Possible protein–RNA interaction sites in these proteins were deduced from previous structural investigations of RNA binding proteins, e.g. glutamine tRNA-synthetase (Rould *et al.*, 1989) and U1 small nuclear ribonucleoprotein A (Nagai *et al.*, 1990). Nevertheless, direct proof for the proposed rRNA contact sites of ribosomal proteins remains to be found. In order to understand the specific interactions through which the complex ribosomal structure is held together, it is challenging to identify the peptide regions of ribosomal proteins that are close to a specific part of the rRNA. Accordingly, in this paper, we have identified the amino acid residues involved in protein–rRNA cross-links by applying a new strategy which allowed us to establish many of the peptide sites of the proteins in close contact with the 16S and 23S RNA. Since no three-dimensional structures are available for the majority of ribosomal proteins, our new data add valuable information about the structural and functional features of peptide regions in ribosomal proteins that are involved in interaction with rRNA.

Results

Size exclusion chromatography

We cross-linked 30S and 50S ribosomal subunits from *Escherichia coli* (Eco) strain MRE600 and *Bacillus stearothermophilus* (Bst) strain 799, either by direct UV irradiation or by treatment with 2-iminothiolane (see Materials and methods) in order to determine the peptides and individual amino acids of ribosomal proteins involved in the interaction with rRNA. We first separated proteins cross-linked to rRNA from the non-cross-linked proteins by size exclusion chromatography on an S300 column. A representative elution profile of cross-linked ribosomal subunits from Bst 30S is given in Figure 1a. The main fractions in the void volume correspond to the rRNA moiety containing cross-linked ribosomal proteins, followed by unbound ribosomal proteins. Control batches of non-cross-linked ribosomal subunits showed the same profile (data not shown). In order to differentiate between cross-linked and unbound proteins, aliquots of the eluted fractions were subjected to SDS–PAGE (Figure 1a). rRNA fractions containing cross-linked proteins were pooled and concentrated for proteolytic digestion. Following proteolytic cleavage of the rRNA pool, a second size exclusion step on the same column followed, to separate cross-

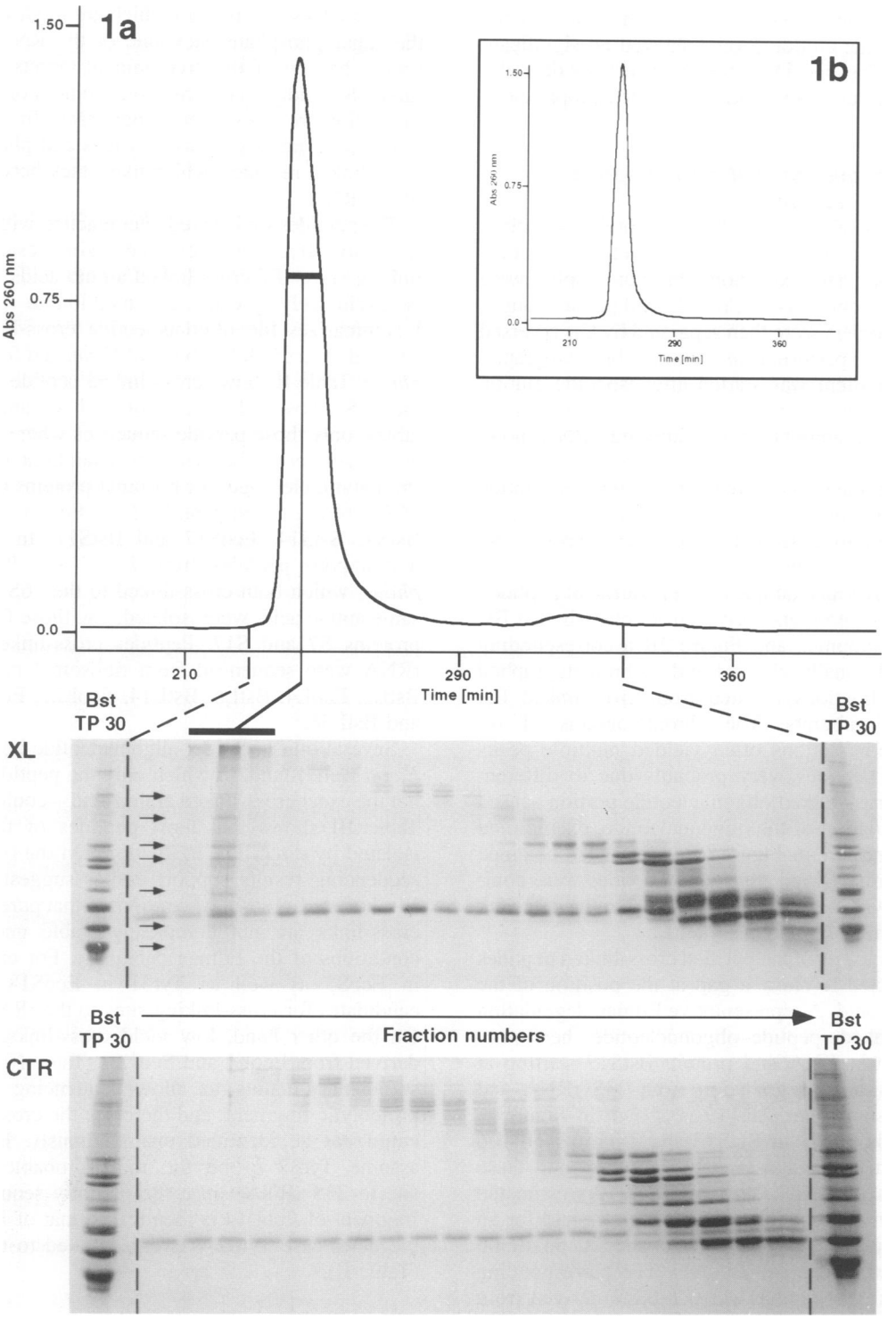

Fig. 1. (**a**) Separation on an S300 column of rRNA–protein cross-linked complexes derived from Bst 30S ribosomal subunits cross-linked with 2-iminothiolane. The upper part of the figure shows the S300 column elution profile of cross-linked Bst 30S ribosomal subunits, and the lower part the SDS–PAGE from aliquots of the corresponding column fractions as indicated by the dashed lines. Direction of elution was from left to right, direction of gel electrophoresis from top to bottom. XL: SDS–PAGE from eluted fractions of cross-linked Bst 30S subunits; CTR: SDS–PAGE from eluted fractions of a control sample with non-cross-linked Bst 30S subunits. The elution profile of non-cross-linked subunits was identical to the cross-linked one (data not shown). For SDS–PAGE, an aliquot of every fifth eluted fraction was precipitated with ethanol. Pellets were redissolved in 25 mM Tris–HCl pH 7.8, 2.5 mM EDTA, incubated with 1 μg RNase A, and loaded onto the gel. Successive fraction numbers are indicated by a long horizontal arrow. Cross-linked proteins are marked with arrows. A band corresponding to RNase A is present in the lower part of each gel slot. Bst TP 30: total protein of 30S subunits from *B.stearothermophilus*. Fractions pooled for further investigations are indicated by black bars in the elution profile and the SDS–PAGE, respectively. (**b**) Separation on an S300 column of rRNA–peptide cross-linked complexes from Bst 30S ribosomal subunits after proteolytic digestion with endoprotease Lys-C.

linked peptides from released ones. With regard to the rRNA fractions, the elution profile showed no significant difference to the first one, indicating no detectable degradation of the rRNA during incubation with the endoproteases (Figure 1b).

RP-HPLC and sequence analysis of peptide–oligonucleotide heteromers

For identification of the cross-linked peptides and their cross-linked amino acids, the rRNA fractions obtained after the second size exclusion chromatography were incubated with ribonucleases. Cross-linked peptide–oligonucleotide heteromers were then separated by C_{18} reversed phase (RP)-high performance liquid chromatography (HPLC). The gradient was started after isocratic elution of the injection peak which varied from 30 to 60 min, depending on the amount of the injected rRNA pool. Fractions which showed absorption at 220 and 260 nm, corresponding to the cross-linked peptide–oligonucleotide moiety, were either applied directly to automated sequencing or submitted to a second proteolytic cleavage and rechromatographed as above.

Figure 2A shows an example of a separation of peptide–oligonucleotide heteromers derived from cross-linked Bst 30S ribosomal subunits, and Figure 2B a corresponding example of additionally cleaved and rechromatographed C_{18} RP-HPLC fractions isolated from cross-linked Bst 50S ribosomal subunits. The chromatograms of rechromatographed fractions often yielded multiple peaks of cross-linked peptides, very probably due to different lengths of the cross-linked oligonucleotide portion caused by partial degradation of the oligonucleotide, exemplified by peaks 1/2 and 3/4 in Figure 2B. Sequences obtained from purified cross-linked ribosomal peptides were compared with known ribosomal sequences from the databank in order to identify the parent protein.

A sequence analysis of the purified cross-linked peptides would be expected to show a gap at the position of the modified amino acid. A representative Edman degradation for a cross-linked peptide–oligonucleotide heteromer derived from 16S rRNA and protein BstS17 starting at Thr21, and a similar degradation from 23S rRNA and protein BstL6 starting at Ala149 is shown in Figure 3. The amino acids Lys31 in BstS17 and Tyr156 in BstL6 are absent in the Edman degradations, confirming these two residues as cross-link sites to rRNA. As estimated from the Edman degradations, the cross-link yield for an individual peptide varies between 20 and 70 pmol/300 A_{260} cross-linked ribosomal subunits. The corresponding yield of cross-linked peptide was 0.2–0.5% derived from 300 A_{260} ribosomal subunits.

Cross-linking sites

We have chosen treatment with 2-iminothiolane followed by direct UV irradiation (Wower *et al.*, 1981) and, alternatively, direct UV irradiation without 2-iminothiolane treatment according to Möller and Brimacombe (1975) for cross-linking ribosomal subunits for two reasons. Firstly, 2-iminothiolane reacts with the primary amines of proteins in the first step (Traut *et al.*, 1973). The resulting thiol group of the derivatized residue can be covalently attached to the RNA in a second step by short UV irradiation. Hence, 2-iminothiolane is a suitable cross-linker for mapping those basic residues of a protein which are in close contact with the sugar phosphate backbone of the RNA, and lysines should be one of the predominant targets for the cross-linker. Secondly, in contrast to 2-iminothiolane, direct UV irradiation produces a zero-length cross-link. We expected aromatic residues such as tyrosines and phenyalanines as cross-linked residues, which may stack between the bases of the RNA.

The peptides we isolated after reaction with 2-iminothiolane most frequently revealed lysine residues as cross-linking sites. UV cross-linked amino acids were found to be exclusively tyrosine and methionine residues. Table I summarizes the oligonucleotide cross-linked peptides isolated from the 30S subunit of *E.coli* and *B.stearothermophilus*, Table II shows cross-linked peptide stretches from the 50S ribosomal subunit of both organisms. In these tables, only those peptide sequences where a cross-linked amino acid could be identified unambiguously are listed. Proteolytic cleavage of ribosomal proteins cross-linked to 16S rRNA revealed peptides from EcoS3, EcoS4, EcoS7, BstS7, BstS14, EcoS17 and BstS17. In several cases, homologous peptides from *E.coli* and *B.stearothermophilus,* which both cross-linked to the 16S rRNA via the same amino acid, were isolated, e.g. those from ribosomal proteins S7 and S17. Peptides cross-linked to the 23S rRNA were sequenced from ribosomal proteins EcoL2, BstL2, EcoL4, BstL6, BstL14, EcoL27, EcoL28, BstL29 and BstL36.

Several other peptide–oligonucleotide heteromers from *E.coli* were found, in which only the peptide stretch—but not the exact cross-linked amino acid—could be identified. Table III shows that most peptides of this type were isolated by direct UV irradiation. On the one hand, these sequencing results support earlier suggestions made by Bischof *et al.* (1994), who proposed that pure photoinduced cross-links are not completely stable under the harsh conditions of the Edman chemistry. For example, Tyr41 in EcoS3 as well as Tyr31 in EcoS18 are potential candidates for cross-linking sites to the rRNA (Table III). On the other hand, low yield cross-links, e.g. peptides derived from EcoL1 and EcoL14 (Table III), did not give sufficient amounts to allow sequencing of the entire proteolytic fragment, and therefore the cross-link position could not be identified unambiguously. In EcoL14 we assume Tyr32 to be the most probable cross-linking site to 23S rRNA, since the partially sequenced peptide fragment of EcoL14 is identical to that of BstL14, and in the latter case Tyr32 was cross-linked to the 23S rRNA (Table II).

Discussion

A new approach (Urlaub *et al.*, 1994) has been developed to determine peptide regions and amino acid residues involved in the interaction with rRNA in intact ribosomal subunits. The method employs HPLC separation of cross-linked peptide–oligonucleotide heteromers followed by direct microsequencing of the peptide moiety. Tables I and II list those peptide–oligonucleotide heteromers of which the cross-linked amino acid residue could be identified unambiguously. In addition, a number of other cross-linked peptides were isolated and purified, where the peptide region could be clearly assigned, but not the amino

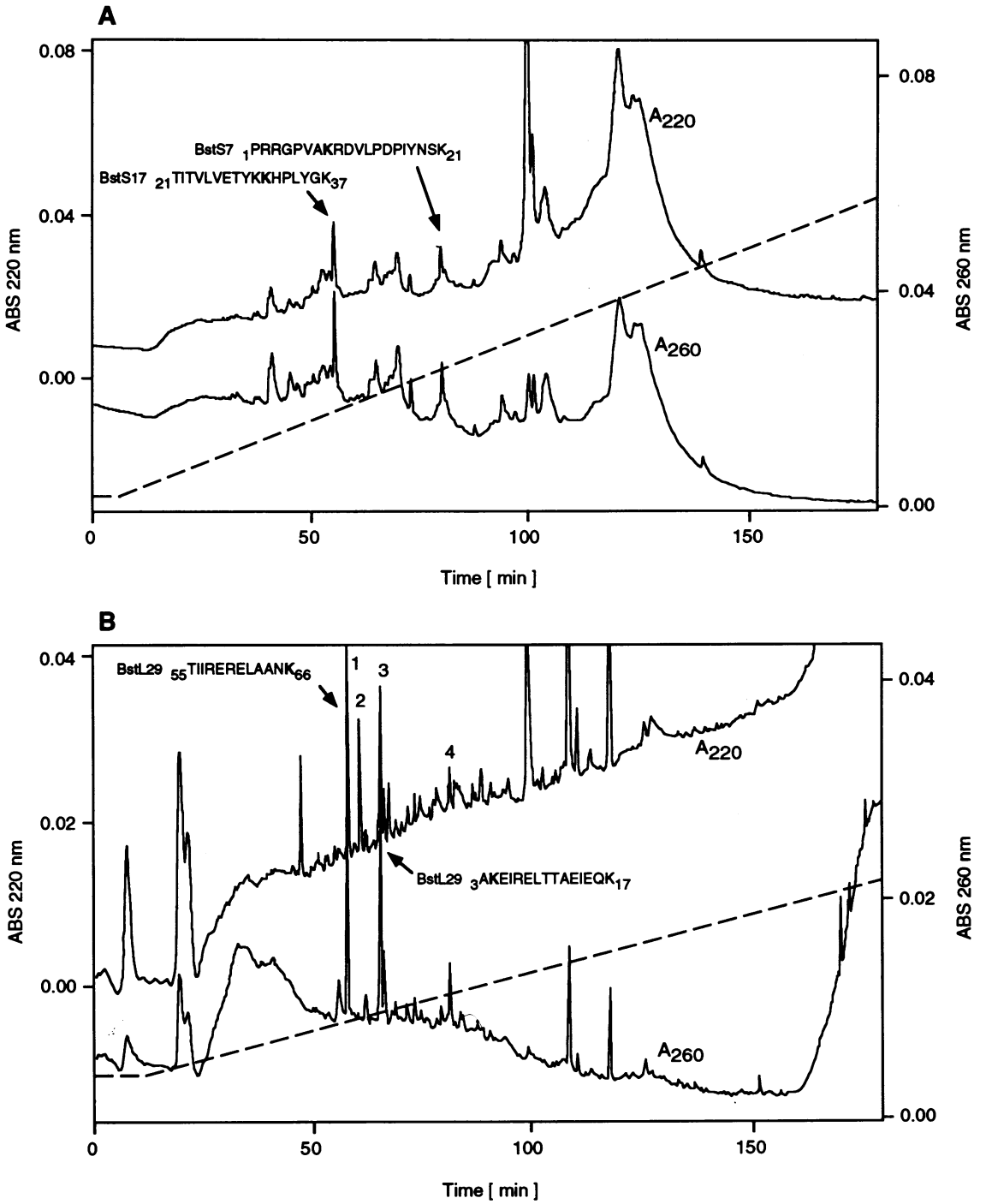

Fig. 2. C_{18} RP-HPLC of cross-linked peptide–oligonucleotide heteromers. (**A**) C_{18} RP-HPLC analysis of peptide–oligonucleotide heteromers derived from Bst 30S cross-linked with 2-iminothiolane. Sample derived from 200 A_{260} of cross-linked Bst 30S treated with RNase T1 and endoprotease Lys-C were injected directly onto a RP-18 LiChrospher® column. The gradient (dashed line) was as follows: 30–60 min isocratic elution with 10% solvent B (0.1% trifluoroacetic acid in acetonitrile) until elution of the injection peak, followed by a gradient of 10–60% buffer B for 180 min and 50–90% buffer B for 30 min. After starting the gradient, the eluate was monitored by a photodiode array detector. Sequences obtained from fractions showing absorption at 220 nm (A_{220}) and 260 nm (A_{260}) are indicated in the chromatogram. Cross-linked amino acids from BstS17 and BstS7 are in bold letters. (**B**) Example of fractions from Bst 50S cross-linked with 2-iminothiolane after a second cleavage with endoprotease Lys-C. Fractions eluted from C_{18} RP-HPLC at a solvent B concentration >40% were treated with endoprotease Lys-C again and rechromatographed. The gradient applied (dashed line) was 10% solvent B for 10 min, 10–50% solvent B in 180 min and 50–90% in 10 min. Absorption was monitored as in (A). Peaks 1 and 2 were identified as C-terminal peptides from BstL29, peaks 3 and 4 as N-terminal peptides from BstL29. Amino acids that were not detected during sequence analysis are shown in bold letters.

acid residue involved in the cross-link (Table III). Such cross-linked peptides were derived mainly from direct UV irradiation, whereas the peptides obtained after 2-iminothiolane treatment in combination with short UV irradiation were found to be stable under the conditions of Edman sequence analysis.

Peptide stretches with amino acids cross-linked to rRNA were identified for 13 different ribosomal proteins from

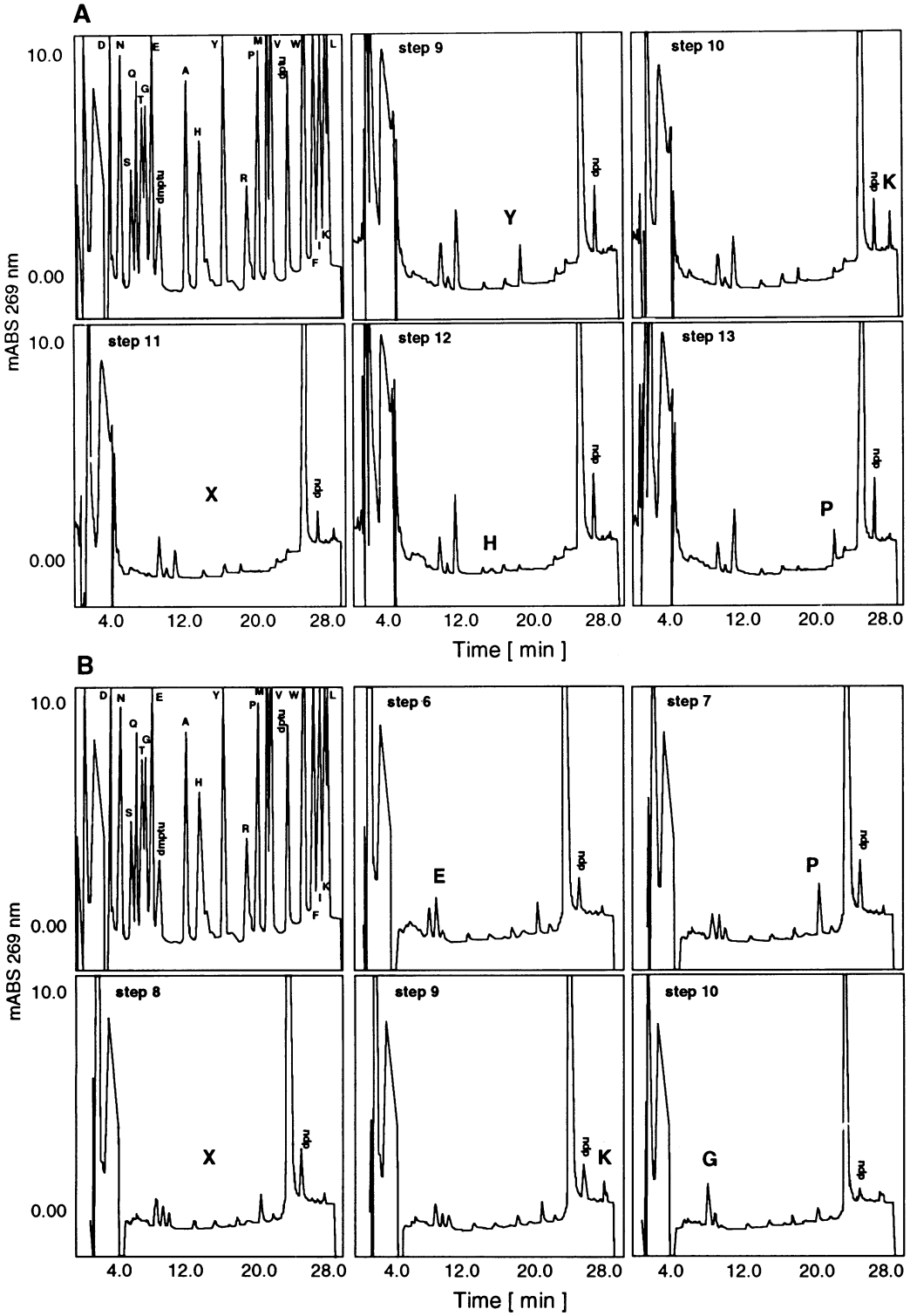

Fig. 3. Sequence analysis of isolated peptide–oligonucleotide cross-links. (**A**) Edman degradation steps of the cross-linked peptide of BstS17, and (**B**) of the cross-linked peptide derived from BstL6. Only degradation steps 9–13 (BstS17) and steps 6–10 (BstL6) are illustrated in the figure. Gaps in the sequence (corresponding to Lys31 of BstS17 in cycle 11 and to Tyr156 of BstL6 in cycle 8, respectively) are indicated with an X. Complete peptide sequences are listed in Tables I and II. The first panel shows the elution profile of the PTH-amino acid standard (each 75 pmol) given in the one-letter code. dmptu is *N,N*-dimethyl-*N'*-phenylthiourea, dptu is diphenylthiourea and dpu is diphenylurea, all of which are Edman degradation by-products.

E.coli and *B.stearothermophilus*. In the following, we will discuss our data with reference to (i) older results obtained from protein–RNA cross-links (e.g. Möller *et al.*, 1978) as well as protein–RNA protection studies (e.g. Watanabe and Kimura, 1985) and (ii) structural information concerning possible rRNA binding sites derived from three-

Table I. Peptides and amino acids cross-linked to 16S rRNA

Ribosomal protein	Reference	Peptide sequence	Cross-link	Cross-linked amino acid
EcoS3	Brauer and Röming, 1979	38VRQYLT**K**ELAK48	2-iminothiolane	Lys44
		86LR**K**VVADIAGVPAQINIAEVRK107	2-iminothiolane	Lys88
EcoS4	Schiltz and Reinbolt, 1975	77EAARL**K**GNTGENLL90	2-iminothiolane	Lys82
EcoS7	Reinbolt *et al.*, 1978	109RGDKSMALRLANELSDAAENK129	UV	Met114
BstS7	Kimura, 1991	1PRRGPVA**K**RDVLPDPIYNSK20	2-iminothiolane	Lys8
		107ARLRGEKTMEERLANEIMDA126	UV	Met115
BstS14	Herfurth *et al.*, 1994	9QKRTPKF**K**VRAYT21	2-iminothiolane	Lys16
EcoS17	Yaguchi and Wittmann-Liebold, 1978	19SIVVAIERFV**K**HPIYGK35	2-iminothiolane	Lys29
BstS17	Herfurth *et al.*, 1991	21TITVLVETYK**K**HPLYGK37	2-iminothiolane	Lys31

Amino acids are in the one-letter code, cross-linked amino acids are in bold letters. Fragment positions are indicated by numbers. Except for the peptide of BstS7 (fragment position 107–126), which was obtained after chymotryptic digestion, all peptides were derived from proteolytic cleavage with endoprotease Lys-C and were isolated by C_{18} RP-HPLC. Large Lys-C fragments did not yield sufficient amounts for complete Edman degradation.

Table II. Peptides and amino acids cross-linked to 23S rRNA

Ribosomal protein	Reference	Peptide sequence	Cross-link	Cross-linked amino acid
EcoL2	Kimura *et al.*, 1982	59QAYRIVDF**K**RNK70	2-iminothiolane	Lys67
		199H**M**LRVLGKA207	UV	Met200
BstL2	Kimura *et al.*, 1985b	238APIGR**K**SPM246	2-iminothiolane	Lys243
EcoL4	Kimura and Wittmann-Liebold, 1980	26ALVHQVVVA**Y**AAGARQGTRAQKTRA50	UV	Tyr35
BstL6	Kimura *et al.*, 1981	149AVRPPEPYKGKGIRY163	UV	Tyr156
BstL14	Kimura *et al.*, 1985a	24VLGGSGRR**Y**ANI35	UV	Tyr32
EcoL27	Chen *et al.*, 1975	66VKFEV**K**GPKNRK77	2-iminothiolane	Lys71
EcoL28	Wittmann-Liebold and Marzinzig, 1977	54GMRVIDK**K**GIDT65	2-iminothiolane	Lys60
BstL29	Kimura *et al.*, 1985a	3A**K**EIRELTTAEIEQK17	2-iminothiolane	Lys4
		55TIIRERELAAN**K**66	2-iminothiolane	Lys66
BstL36	Tanaka *et al.*, 1984	14C**K**VIRRRGKVMVICENPK31	2-iminothiolane	Lys15

Amino acids are in the one-letter code, cross-linked amino acids are in bold letters, numbers indicate the fragment positions. Peptides of EcoL2 (fragment position 199–207) and EcoL4 were obtained after digestion with endoprotease Glu-C, the peptide of BstL6 after proteolytic cleavage with chymotrypsin. All other peptides were derived from digestion with endoprotease Lys-C and subsequent C_{18} RP-HPLC. As noted for the peptides in Table I, large Lys-C fragments could not be sequenced to the C-terminus, as well as the EcoL2 and EcoL4 Glu-C fragments.

Table III. Peptide stretches cross-linked to the rRNA, in which no cross-linked amino acid could be identified

Ribosomal protein	Reference	Peptide sequence	Cross-link
EcoS2	Wittmann-Liebold and Bosserhoff, 1981	26MKPFIFGAR34	UV
EcoS3	Brauer and Röming, 1979	38VRQYLTK44	UV
EcoS9	Chen and Wittmann-Liebold, 1975	120ARRRPQFSKR129	UV
EcoS12	Funatsu *et al.*, 1977	1ATVNQLVRKP10	UV
EcoS18	Yaguchi, 1975	30NYITESGK37	UV
EcoS21	Vandekerckhove *et al.*, 1975	25AGVLAEVRRR34	UV
EcoL1	Brauer and Öchsner, 1978	198AKPTQ202	UV
BstL4	Herwig *et al.*, 1992	53NRAEVSGGGRKP64	2-iminothiolane
		66RQKGTGRARQ75	2-iminothiolane
EcoL14	Moringa *et al.*, 1978	24VLGGS28	UV

All peptides derived from endoproteolytic cleavage with Lys-C (exept peptide from BstL4, positions 66–75, which was obtained after cleavage with chymotrypsin) followed by elution on a C_{18} RP-HPLC. Fragment positions are given. Only peptides from EcoS3 and EcoS18 could be sequenced completely to the C-terminus (see Results).

dimensional models of ribosomal proteins (Golden *et al.*, 1993a,b). Furthermore, we compare our data with antibiotic binding sites and amino acid residues in ribosomal proteins that are responsible for antibiotic resistance phenomena (Bischof *et al.*, 1994).

For all those proteins for which we identified peptides and amino acids cross-linked to rRNA, corresponding cross-linking sites on the rRNA have been established (for review, see Brimacombe, 1991). For ribosomal proteins EcoS7 and EcoL4, the amino acids cross-linked to rRNA via UV irridation had also been determined (Ehresmann *et al.*, 1976; Möller *et al.*, 1978, Met114 in EcoS7 cross-linked to oligonucleotides 1238–1243 on 16S rRNA; Maly *et al.*, 1980, Tyr35 in EcoL4 cross-linked to oligonucleotides 613–616 on 23S rRNA). Additionally, EcoS7 has been cross-linked with 2-iminothiolane to a second site on the 16S rRNA at nucleotides 1377–1378 (Wower and Brimacombe, 1983). This position is located close to the decoding region of the 16S rRNA and has been suggested to be involved in the formation of the A and P site (Döring

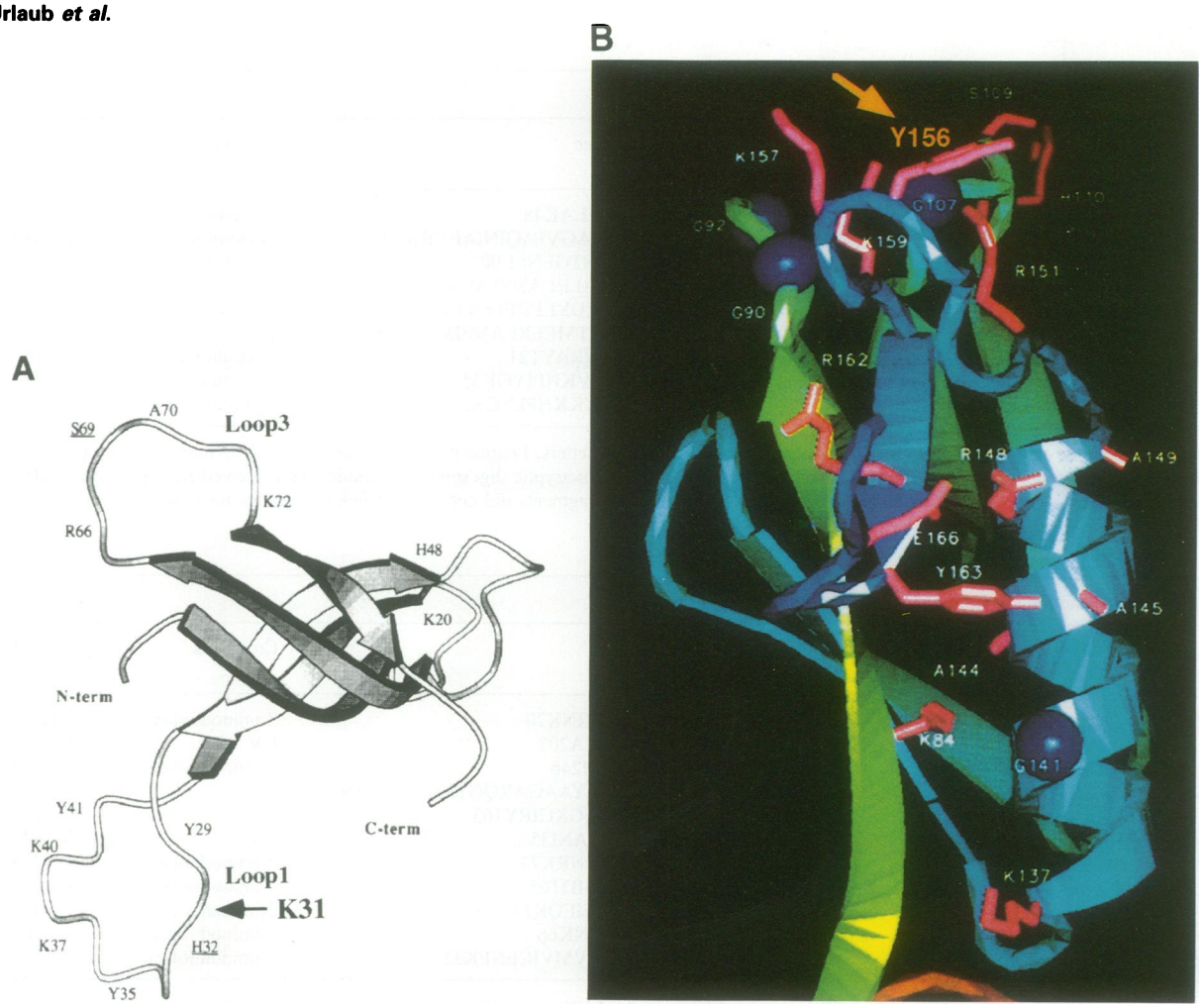

Fig. 4. Three-dimensional structure of ribosomal protein BstS17 (**A**) and of the proposed rRNA-interacting domain of BstL6 (**B**) modified from Golden *et al.* (1993a,b). Amino acids cross-linked to rRNA are indicated by arrows (this work).

et al., 1994). The data generated by our approach clearly confirm the protein domains around these conserved residues, namely at Met114 in EcoS7 and in BstS7 (Met115), as being rRNA-interacting regions. Accordingly, the second cross-link site in the well conserved N-terminal area of this protein in *B.stearothermophilus* derived after treatment with 2-iminothiolane provides evidence for a second site of interaction between rRNA and protein S7 in the decoding region. This hypothesis is strongly supported by affinity labelling of puromycin to the same N-terminal region (Bischof *et al.*, 1994), as puromycin binds in the ribosomal A site.

In EcoL2 and EcoS4, we were able to localize well defined peptides cross-linked to rRNA (positions 59–70 and 199–207 in EcoL2; position 77–90 in EcoS4). The peptides are all situated within extended central domains proposed to interact with rRNA, as determined by protein protection analysis of EcoS4 and BstL2 (Newberry *et al.*, 1977; Watanabe and Kimura, 1985). Deletion of a region from EcoL2 containing the cross-linked peptide close to the C-terminus results in the inability of this protein to assemble into functional 50S subunits (Romero *et al.*, 1990), and therefore supports the structural importance of the cross-linked peptide regions for ribosomal function.

Comparison with the three-dimensional structures of ribosomal proteins

The amino acids of BstS17 (Lys31) and BstL6 (Tyr156) cross-linked to rRNA are located within the loop regions of the proteins which are proposed to interact with rRNA (Golden *et al.*, 1993a,b, see Figure 4A and B). Furthermore, the isolation of homologous peptides of EcoS17 (Lys29 cross-linked) and of ribosomal protein S17 from *Halo-arcula marismortui* (Lys62 cross-linked; Klußmann, unpublished data) cross-linked to rRNA implicate an identical structural feature of the contact sites between rRNA and proteins in these organisms. Crystallographic data of BstL14 (S.W.White, personal communication) place the cross-linked Tyr32 also in an exposed loop structure. Thus, our new data directly demonstrate, for the first time, the contact sites of ribosomal proteins on the rRNA in the three-dimensional models.

RNA binding structural elements

The cross-linked peptide stretches and their adjacent regions consist predominantly of basic residues and hydrophobic amino acids (see Tables I, II and III). From studies on nucleic acid binding proteins (Ollis and White, 1987) and of crystallized small RNA binding proteins (Nagai

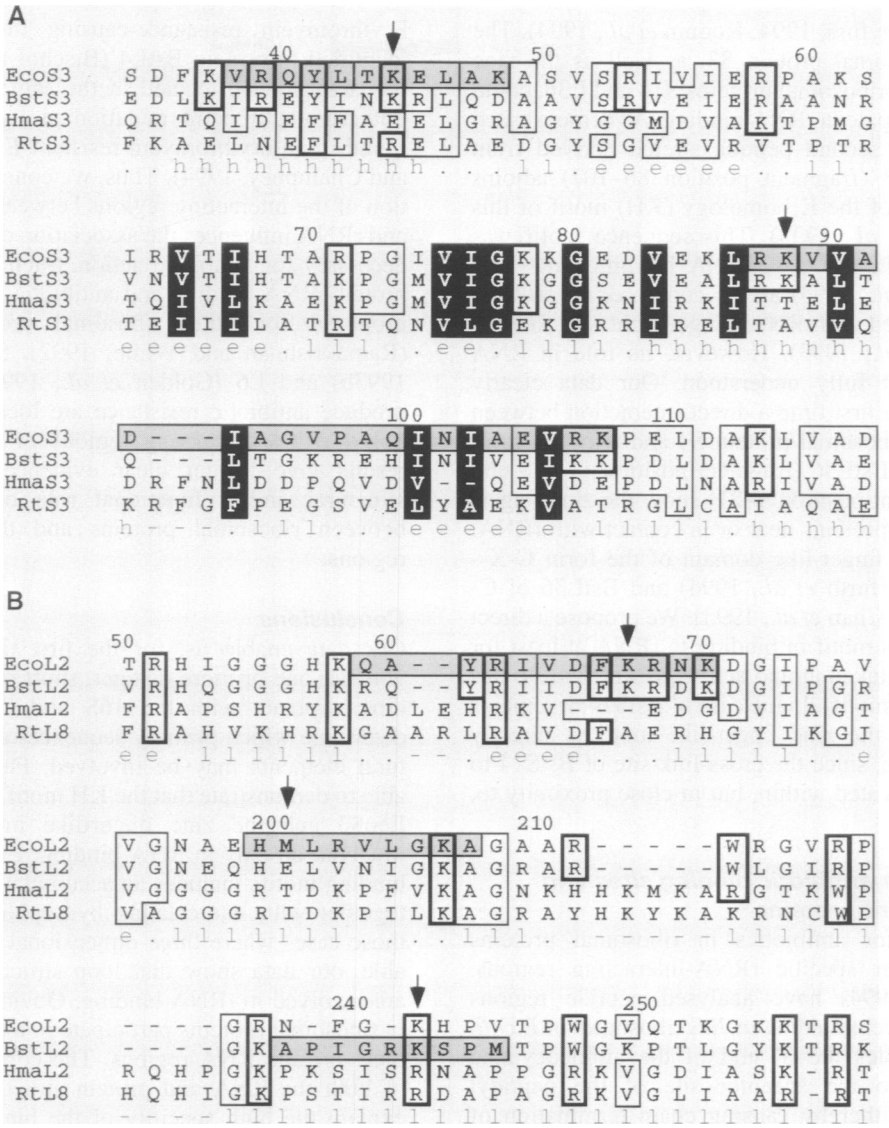

Fig. 5. Alignment of selected sequences of protein EcoS3 (**A**) and protein EcoL2 (**B**) to homologous proteins from other ribosomes. Amino acids are given in the one-letter code. Identical residues are boxed, conserved basic and aromatic residues are heavily outlined. Conserved residues of the KH motif (Gibson *et al.*, 1993) in the protein S3 family are shown by white letters in black outlines (A). Multiple sequence analyses were performed with PILEUP and PRETTYPLOT (Genetics Computer Group, Wisconsin, USA, 1991) and secondary prediction analysis with PHDsec (Rost and Sander, 1994a,b). Abbreviations are as follows: Eco, *E.coli*; Bst, *B.stearothermophilus*; Hma, *H.marismortui*; Rt, rat; e, β-strand; h, helix; l, loop. Isolated cross-linked peptide stretches are boxed and shaded. Amino acids cross-linked to the rRNA are indicated by an arrow. Numbering of the amino acid residues refers to the *E.coli* protein.

et al., 1990; Hoffman *et al.*, 1991; Ramakrishnan and White, 1992; Golden *et al.*, 1993b; Hoffman *et al.*, 1994), it was proposed that rRNA binding sites consist of conserved basic residues such as lysines and arginines interacting with the sugar phosphate backbone of rRNA. Exposed aromatic residues such as tyrosines may intercalate between the bases of rRNA, and small hydrophobic amino acids permit close contacts to the rRNA. This assumption has been strongly confirmed by the crystal structure analysis of U1A protein complexed with an RNA hairpin (Oubridge *et al.*, 1994). In the three-dimensional structure of the proteins crystallized so far, all these above mentioned residues are located within loop structures flanked by conserved β-strands (which, for example, harbour the RNA binding motif, RNP, in small nuclear RNA binding proteins). After secondary structure prediction according to Rost and Sander (1994a,b) on the ribosomal proteins involved in cross-linking to the rRNA, we observed a similar feature of loops and β-strands for the cross-linked peptide regions from proteins EcoL2, BstL4, BstL14, EcoL27, EcoS3 (Lys44 cross-linked), BstS7 (Lys8 cross-linked) and BstS14. As shown in Figure 5A and B for S3 (Lys44 cross-linked) and L2 (Lys67 cross-linked), the cross-linked basic amino acids are positioned in or near a loop region. The adjacent conserved β-strands contain hydrophobic as well as aromatic residues. Even though other cross-linked peptide stretches do not share this feature, they are in close proximity to such regions (e.g. EcoL4, Tyr35 cross-linked; EcoS4, Lys82 cross-linked; EcoS7 and BstS7, Met144 and Met115 cross-linked, respectively).

A sequence comparison of all ribosomal peptides involved in interaction with the rRNA was performed for known primary RNA binding sequence motifs (e.g. Mattaj,

1993; Burd and Dreyfuss, 1994; Koonin *et al.*, 1994). The KH motif of ribosomal protein S3, as well as the zinc finger-like motif of ribosomal proteins S14 and L36, could be proven to participate in rRNA binding. As demonstrated in Figure 5A, the second peptide stretch derived from cross-linked EcoS3 (fragment position 86–107) adjoins the core sequence of the K homology (KH) motif of this protein (Gibson *et al.*, 1993). This sequence motif was first identified in human pre-mRNA binding hnRNP K protein (Siomi *et al.*, 1993) and is conserved in proteins which are associated with RNA (Engebrecht and Roeder, 1990; Gibson *et al.*, 1993). However, its role in RNA binding is not yet fully understood. Our data clearly demonstrate for the first time a direct interaction between the KH motif of ribosomal protein S3 and rRNA. Cross-linked peptides of BstL36 (fragment position 14–36) and of BstS14 (fragment position 9–21) show the zinc finger-like motif of these proteins near or in contact with rRNA. BstS14 has a zinc finger-like domain of the form C-X_2-C-X_{12}-C-X_2-C (Herfurth *et al.*, 1994) and BstL36 of C-X_2-C-X_{12}-C-X_4-H (Chan *et al.*, 1993). We propose a direct participation of this motif in binding to rRNA at least for BstL36 (the cross-linked amino acid Lys15 of BstL36 lies within the putative motif). In the case of BstS14, it remains uncertain whether the zinc finger-like motif is directly involved in binding, since the cross-link site of BstS14 to the rRNA is not located within, but in close proximity to, this motif.

Comparison with antibiotic binding sites and antibiotic-resistant proteins

Accessible sites for antibiotics in ribosomal proteins coincide with their specific rRNA-interacting regions. Bischof *et al.* (1994) have analysed peptide regions involved in puromycin binding in 70S ribosomes of *E.coli*. Puromycin resembles the 3′ end of the aminoacylated tRNA. It binds to the acceptor site of the peptidyl transferase centre, thereby causing chain termination of the nascent polypeptide chain. Identical cross-linking sites to puromycin and to the rRNA were found in the N-terminal domain of protein S7 (see above), in protein S14 (position 9–21 cross-linked to rRNA in *B.stearothermophilus*) and in L29 (position 55–66 cross-linked to rRNA in *B.stearothermophilus*). The structural role of these protein regions as part of the decoding region and the peptidyl transferase centre, respectively, has already been discussed critically (Bischof *et al.*, 1994). Affinity labelling of ribosomal proteins with the antibiotic spiramycin (Bischof *et al.*, 1995), which belongs to the group of macrolides and acts as peptidyl transferase inhibitor, gave rise to the same labelled peptide stretch of EcoS12 and EcoL27, which we identified as major cross-linking sites to the rRNA. Spiramycin also interacts with S14 in *E.coli* within the domain homologous to that cross-linked to rRNA in *B.stearothermophilus*.

Mutations in ribosomal proteins EcoL4 and BstL4 close to or within the region cross-linked to the rRNA lead to resistance to the antibiotic erythromycin and to a dramatic loss of peptidyl transferase activity. The N-terminal regions of EcoL4 (position 26–50) and BstL4 (positions 53–64 and 66–75) are the predominant cross-linking sites to the 23S rRNA, determined either by direct UV irradiation (EcoL4) or by treatment with 2-iminothiolane (BstL4). Erythromycin resistance-causing mutations, that were identified in protein BstL4 (Bischof *et al.*, manuscript in preparation), are located in the same N-terminal region. Futhermore, a point mutation at Lys63 in EcoL4 was found in an erythromycin-resistant *E.coli* strain (Chittum and Champney, 1994). Thus, we conclude that a perturbation of the interacting regions between ribosomal proteins and rRNA influences the association of neighbouring parts necessary for antibiotic action. Such correlation between protein–RNA binding and antibiotic interaction has been proposed for other ribosomal proteins such as S5 (Ramakrishnan and White, 1992), S17 (Golden *et al.*, 1993b) and L6 (Golden *et al.*, 1993a). Mutations that produce antibiotic resistance are located within the proposed rRNA-interacting regions of these proteins. Our results give further clear evidence for the important structural and/or functional role of the contact sites between ribosomal proteins and their specific rRNA regions.

Conclusions

Our data enable us, for the first time, to differentiate whether one or more distinct, short protein regions are in direct contact with the 16S and 23S rRNAs, and to determine which primary sequences and secondary structural elements may be involved. Furthermore, we were able to demonstrate that the KH motif of ribosomal protein EcoS3 and the zinc finger-like motif of BstL36 are involved directly in RNA binding. Evidence for common binding motifs includes an accumulation of basic residues together with intercalating hydrophobic amino acids. In those cases where three-dimensional structures are available, our data show that loop structures of the proteins are involved in rRNA binding. Obviously, loop structures in ribosomal proteins participate in a tight interaction with their specific RNA regions. The conformational changes of both the RNA and protein structural elements might explain the high specifity of the binding of the proteins to the RNA.

Materials and methods

All chemicals used were p.A. grade or ultra pure, obtained from Merck (Darmstadt, Germany) or GIBCO BRL (Gaithersburg, MD). Endoproteases Lys-C (EC 3.4.99.30), Glu-C (EC 3.4.21.19), chymotrypsin (EC 3.4.21.1) and RNase A were purchased from Boehringer Mannheim (Mannheim, Germany). RNase T1 was obtained from Calbiochem (San Diego, CA) and 2-iminothiolane (Traut's reagent) from Pierce (Rockford, USA).

Preparation of ribosomes

Cells of *E.coli* strain MRE600 and of *B.stearothermophilus* strain 799 were grown and ribosomal subunits isolated by sucrose gradient centrifugation, as described by Brockmöller and Kamp (1986). For the cross-linking reaction induced by UV irradiation, 3000 A_{260} of ribosomal subunits were dialysed extensively against 10 mM Tris–HCl pH 7.8, 50 mM KCl, 5 mM magnesium acetate and 6 mM 2-mercaptoethanol, and then diluted with the same buffer to a concentration of 5 A_{260}/ml. For chemical cross-linking with 2-iminothiolane, 3000 A_{260} of ribosomal subunits were dialysed extensively against the same buffer (containing 25 mM triethanolamine-HCl pH 7.8 instead of Tris) and then adjusted to a concentration of 20 A_{260}/ml.

UV and chemical cross-linking of ribosomal subunits

UV cross-linking was carried out at 4°C for 10 min at 254 nm (G8T5 8W, GERMICIDAL Lamps, Herolab, Wiesloch, Germany) at a distance of 5 cm. Glass dishes with an inner diameter of 12.5 cm were used. The

ribosomal solution had a depth of ~1 mm (Möller and Brimacombe, 1975). Cross-linking with 2-iminothiolane was carried out according to Wower *et al.* (1981), and UV activation of the modified ribosomal subunits was performed at a concentration of 5 A_{260}/ml for 2 min as described for UV cross-linking. Cross-linked ribosomal subunits were precipitated with two volumes of 98% ethanol and 1/10 volume of 1 M sodium acetate pH 6.8 for 2 h at –20°C, and centrifuged in a HB6 at 10 000 r.p.m. for 30 min. The pellet was washed with 80% ethanol, centrifuged for 15 min as above, and redissolved in 25 mM Tris–HCl pH 7.8, 2 mM EDTA, 6 mM 2-mercaptoethanol and 0.1% SDS (buffer A) at a concentration of 100 A_{260}/ml. Cross-linked ribosomal subunits were stored at –80°C.

Size exclusion chromatography

Ribosomal proteins cross-linked to rRNA were separated from the non-cross-linked proteins by size exclusion chromatography on an S300 column (Pharmacia LKB, Biotechnologie, Uppsala, Sweden, 2.6× 100 cm) running in buffer A (see above) with a flow rate of 0.7 ml/min. Proteins cross-linked to rRNA were identified by SDS–PAGE (Laemmli, 1970). rRNA fractions containing proteins were pooled, precipitated with ethanol, centrifuged as described above and redissolved in an appropriate volume of 25 mM Tris–HCl pH 7.8, 0.1% SDS, including 40 units of RNasin/ml buffer. Proteolytic fragmentations of cross-linked ribosomal proteins were carried out for 16 h at 37°C with an enzyme to substrate ratio of 1.3×10^{-3} units endoprotease Lys-C to 1.0 A_{260}, 0.01 µg endoprotease Glu-C to 1.0 A_{260} and 0.01 µg endoprotease chymotrypsin to 1.0 A_{260}. Finally, the remaining cross-linked peptides were separated from released peptides by size exclusion chromatography as described above. Fractions containing rRNA were collected, precipitated with ethanol, washed and stored at –20°C at a concentration of 200 A_{260}/ml in 25 mM Tris–HCl pH 7.8 and 2.5 mM EDTA.

C_{18} RP-HPLC

For purification of the cross-linked peptide–oligonucleotide heteromers, aliquots derived from 200–300 A_{260}, rRNA–peptide cross-links were either completely digested with RNase A and T1 at a concentration of 0.01 µg nuclease/A_{260} for 1 h 55°C or treated with RNase T1 in the same manner. Digestion was stopped by injection onto a HPLC 100 RP-18 LiChrospher® endcapped column (250×4 mm, 5 µm, E.Merck, Darmstadt, Germany) or onto a Vydac C_{18} column (250×4 mm or 250×4.6 mm, 5 µm, The separations group, Hesperia, CA) at a flow rate of 0.5 ml/min at 22°C. Solvent A was water with 0.1% trifluoroacetic acid and solvent B was acetonitrile with 0.1% trifluoroacetic acid. Fractions which showed an absorbance at 220 and 260 nm were sequenced in a Model 477A pulsed-liquid phase sequencer equipped with a Model 120A amino acid analyser (Applied Biosystems Inc., Foster City, USA). Fractions which eluted at higher buffer B concentrations (40–60%) from the column were collected, dried under vacuum and redissolved in 100 mM Tris–HCl pH 8.0, 10% acetonitrile and 1% hydrogenated Triton X-100. Proteolytic cleavage of these fractions was carried out with 1 µg of endoprotease Lys-C (sequencing grade) for 16 h at 37°C. Subsequent to proteolytic digestion, the fractions were rechromatographed as above.

Computer analysis

The NBRF databank (National Biomedical Research Foundation, Washington DC) or the RIBO databank (MDC, Proteinchemistry Group, Berlin, Germany) were used for sequence comparison by FASTA (Genetics Computer Group, Wisconsin, USA, 1991). Multiple sequence analysis was done with the programs PILEUP and PRETTYPLOT (Genetics Computer Group, Wisconsin, USA, 1991). Prediction of secondary structure of ribosomal proteins was performed via PHDsec (Rost and Sander, 1994a,b).

Acknowledgements

We thank Dr Richard Brimacombe for critically reading the manuscript and Dr Stephen W.White for providing unpublished data. This work was supported by a grant to Dr B.W.-L. from the Deutsche Forschungsgemeinschaft (SFB 344, YE6).

References

Bergmann,U. and Wittmann-Liebold,B. (1993) Identification of cross-linked amino acids in the protein pair HmaL23–HmaL29 from the 50S ribosomal subunit of the archaebacterium *Haloarcula marismortui*. *Biochemistry*, **32**, 2880–2887.

Bischof,O., Kruft,V. and Wittmann-Liebold,B. (1994) Analysis of the puromycin binding site in the 70S ribosome of *Escherichia coli* at the peptide level. *J. Biol. Chem.*, **229**, 18315–18319.

Bischof,O., Urlaub,H., Kruft,V. and Wittmann-Liebold,B. (1995) Peptide environment of the peptidyl transferase center from *Escherichia coli* 70S ribosomes as determined by thermo affinity labeling with dihydrospiramycin. *J. Biol. Chem.*, in press.

Brauer,D. and Öchsner,I. (1978) The primary structure of protein L1 from the large ribosomal subunit of *Escherichia coli*. *FEBS Lett.*, **96**, 317–321.

Brauer,D. and Röming,R. (1979) The primary structure of protein S3 from the small ribosomal subunit of *Escherichia coli*. *FEBS Lett.*, **106**, 352–357.

Brimacombe,R. (1991) RNA–protein interactions in the *Escherichia coli* ribosome. *Biochimie*, **73**, 927–936.

Brockmüller,J. and Kamp,R.M. (1986) Isolation and identification of two protein–protein crosslinks within the two subunits of *Bacillus stearothermophilus* ribosomes. *Biol. Chem. Hoppe-Seyler's*, **367**, 925–935.

Brockmöller,J. and Kamp,R.M. (1988) Cross-linked amino acids in the protein pair S13–S19 and sequence analysis of protein S13 of *Bacillus stearothermophilus* ribosomes. *Biochemistry*, **27**, 3372–3381.

Burd,C.G. and Dreyfuss,G. (1994) Conserved structures and diversity of functions of RNA-binding proteins. *Science*, **265**, 615–621.

Chan,Y.-L., Suzuki,K., Olvera,J. and Wool,I.G. (1993) Zinc-finger-like motifs in rat ribosomal proteins S27 and S29. *Nucleic Acids Res.*, **21**, 649–655.

Chen,R. and Wittmann-Liebold,B. (1975) The primary structure of protein S9 from the 30S subunit of *Escherichia coli* ribosomes. *FEBS Lett.*, **52**, 139–140.

Chen,R., Mende,L. and Arfsten,U. (1975) The primary structure of protein L27 from the peptidyl-tRNA binding site of *Escherichia coli* ribosomes. *FEBS Lett.*, **59**, 96–99.

Chittum,H.S. and Champney,W.S. (1994) Ribosomal protein gene sequence changes in erythromycin-resistant mutants of *Escherichia coli*. *J. Bacteriol.*, **176**, 6192–6198.

Döring,T., Mitchell,P., Osswald,M., Bochkariov,D. and Brimacombe,R. (1994) The decoding region of 16S RNA: a cross-linking study of the ribosomal A, P and E sites using tRNA derivatized at position 32 in the anticodon loop. *EMBO J.*, **13**, 2677–2685.

Ehresmann,B., Reinbolt,J., Backendorf,C., Tritsch,D. and Ebel,J.P. (1976) Studies of the binding sites of *Escherichia coli* ribosomal protein S7 with 16S RNA by ultraviolet irradiation. *FEBS Lett.*, **67**, 316–319.

Engebrecht,J. and Roeder,G.S. (1990) *MER1*, a yeast gene required for chromosome pairing and genetic recombination, is induced in meiosis. *Mol. Cell. Biol.*, **10**, 2379–2389.

Funatsu,G., Yaguchi,M. and Wittmann-Liebold,B. (1977) Primary structure of protein S12 from the small *Escherichia coli* ribosomal subunit. *FEBS Lett.*, **73**, 12–17.

Gibson,T.J., Thompson,J.D. and Heringa,J. (1993) The KH domain occurs in a diverse set of RNA-binding proteins that include the antiterminator NusA and is probably involved in binding to nucleic acid. *FEBS Lett.*, **324**, 361–366.

Golden,B.L., Ramakrishnan,V. and White,S.W. (1993a) Ribosomal protein L6: structural evidence of gene duplication from a primitive RNA binding protein. *EMBO J.*, **12**, 4901–4908.

Golden,B.L., Hoffman,D.W., Ramakrishnan,V. and White,S.W. (1993b) Ribosomal protein S17: characterization of the three-dimensional structure by ^{1}H and ^{15}N NMR. *Biochemistry*, **32**, 12812–12820.

Herfurth,E., Hirano,H. and Wittmann-Liebold,B. (1991) The amino-acid sequence of the *Bacillus stearothermophilus* ribosomal protein S17 and S21 and their comparison to homologous proteins of other ribosomes. *Biol. Chem. Hoppe-Seyler's*, **372**, 955–961.

Herfurth,E., Briesemeister,U. and Wittmann-Liebold,B. (1994) Complete amino acid sequence of ribosomal protein S14 from *Bacillus stearothermophilus* and homology studies to other ribosomal proteins. *FEBS Lett.*, **351**, 114–118.

Herwig,S., Kruft,V. and Wittmann-Liebold,B. (1992) Primary structures of ribosomal proteins L3 and L4 from *Bacillus stearothermophilus*. *Eur. J. Biochem.*, **207**, 877–885.

Herwig,S., Kruft,V., Eckart,K. and Wittmann-Liebold,B. (1993) Cross-linked amino acids in the protein pairs L3–L19 and L23–L29 of *Bacillus stearothermophilus* ribosomes after treatment with diepoxybutane. *J. Biol. Chem.*, **268**, 4643–4650.

Hoffman,D.W., Query,C.C., Golden,B.L., White,S.W. and Keene,J.D.

(1991) RNA-binding domain of the A protein component of the U1 small nuclear ribonucleoprotein analyzed by NMR spectroscopy is structurally similar to ribosomal proteins. *Proc. Natl Acad. Sci. USA*, **88**, 2495–2499.

Hoffman,D.W., Davies,C., Gerchman,S.E., Kycia,J.H., Porter,S.J., White, S.W. and Ramakrishnan,V. (1994) Crystal structure of prokaryotic ribosomal protein L9: a bi-lobed RNA-binding protein. *EMBO J.*, **13**, 205–212.

Kimura,M. (1991) The nucleotide sequence of *Bacillus stearothermophilus* ribosomal protein S12 and S7 genes: comparison with the str operon of *Escherichia coli*. *Agric. Biol. Chem.*, **55**, 207–213.

Kimura,M. and Wittmann-Liebold,B. (1980) The primary structure of protein L4 from the large subunit of the *Escherichia coli* ribosome. *FEBS Lett.*, **121**, 317–322.

Kimura,M., Rawlings,N. and Appelt,K. (1981) The amino acid sequence of protein BL10 from the 50S subunit of the *Bacillus stearothermophilus* ribosome. *FEBS Lett.*, **136**, 58–64.

Kimura,M., Mende,L. and Wittmann-Liebold,B. (1982) The primary structure of protein L2 from the *Escherichia coli* ribosome. *FEBS Lett.*, **149**, 304–312.

Kimura,M., Kimura,J. and Ashman,K. (1985a) The complete primary structure of ribosomal proteins L1, L14, L15, L23, L24 and L29 from *Bacillus stearothermophilus*. *Eur. J. Biochem.*, **150**, 491–497.

Kimura,M., Kimura,J. and Watanabe,K. (1985b) The primary structure of ribosomal protein L2 from *Bacillus stearothermophilus*. *Eur. J. Biochem.*, **153**, 289–297.

Koonin,E.V., Bork,P. and Sander,C. (1994) A novel RNA-binding motif in omnipotent suppressors of translation termination, ribosomal proteins and a ribosome modification enzyme? *Nucleic Acids Res.*, **22**, 2166–2167.

Laemmli,U.K. (1970) Cleavage of structural proteins during the assembly of the head of bacteriophage T4. *Nature*, **227**, 680–685.

Leijonmarck,M., Eriksson,S. and Liljas,A. (1980) Crystal structure of a ribosomal component at 2.6 Å resolution. *Nature*, **286**, 824–826.

Lindahl,M. *et al.* (1994) Crystal structure of the ribosomal protein S6 from *Thermus thermophilus*. *EMBO J.*, **13**, 1249–1254.

Maly,P., Rinke,J., Ulmer,E., Zwieb,C. and Brimacombe,R. (1980) Precise localisation of the site of cross-linking between protein L4 and 23S ribonucleic acid induced by mild ultraviolet irradiation of *Escherichia coli* 50S ribosomal subunits. *Biochemistry*, **19**, 4179–4188.

Mattaj,I.W. (1993) RNA recognition: a family matter? *Cell*, **73**, 837–840.

Möller,K. and Brimacombe,R. (1975) Specific cross-linking of proteins S7 and L4 to ribosomal RNA, by UV irradiation of *Escherichia coli* ribosomal subunits. *Mol. Gen. Genet.*, **141**, 343–355.

Möller,K., Zwieb,C. and Brimacombe,R. (1978) Identification of the oligonucleotide and oligopeptide involved in an RNA–protein crosslink induced by ultraviolet irradiation of *Escherichia coli* 30S ribosomal subunits. *J. Mol. Biol.*, **126**, 489–506.

Moringa,T., Funatsu,G., Funatsu,M., Wittmann-Liebold,B. and Wittmann,H.G. (1978) Primary structure of protein L14 from *Escherichia coli* ribosomes. *FEBS Lett.*, **91**, 74–77.

Nagai,K., Oubridge,C., Jessen,T.H., Li,J. and Evans,P.R. (1990) Crystal structure of the RNA-binding domain of the U1 small nuclear ribonucleoprotein A. *Nature*, **348**, 515–520.

Newberry,V., Yaguchi,M. and Garrett,R.A. (1977) A trypsin-resistant fragment from complexes of ribosomal protein S4 with 16-S RNA of *Escherichia coli* and from uncomplexed protein. *Eur. J. Biochem.*, **76**, 51–61.

Ollis,D.L. and White,S.W. (1987) Structural basis of protein–nucleic acid interactions. *Chem. Rev.*, **87**, 981–995.

Oubridge,C,. Ito,N., Evans,P.R., Teo,C.-H. and Nagai,K. (1994) Crystal structure at 1.92 Å resolution of the RNA-binding domain of the U1A sliceosomal protein complexed with an RNA hairpin. *Nature*, **372**, 432–438.

Pohl,T. and Wittmann-Liebold,B. (1988) Identification of a cross-link in the *Escherichia coli* ribosomal protein pair S13–S19 at the amino acid level. *J. Biol. Chem.*, **263**, 4293–4301.

Ramakrishnan,V. and White,S.W. (1992) The structure of ribosomal protein S5 reveals sites of interaction with 16S rRNA. *Nature*, **358**, 768–771.

Reinbolt,J., Tritsch,D. and Wittmann-Liebold,B. (1978) The primary structure of ribosomal protein S7 from *Escherichia coli* strains K and B. *FEBS Lett.*, **91**, 297–301.

Romero,D.P., Arrendondo,J.A. and Traut,R.R. (1990) Identification of a region of *Escherichia coli* ribosomal protein L2 required for the assembly of L16 into the 50S ribosomal subunit. *J. Biol. Chem.*, **30**, 18185–18191.

Rost,B. and Sander,C. (1994a) Combining evolutionary information and neural networks to predict protein secondary structure. *Proteins*, **19**, 55–77.

Rost,B. and Sander,C. (1994b) PHD— a mail server for protein secondary structure prediction. *CABIOS*, **10**, 53–60.

Rould,M.A., Perona,J.J., Söll,D. and Steitz,T.A. (1989) Structure of *E.coli* glutaminyl-tRNA synthetase complexed with $tRNA^{Gln}$ and ATP at 2.8 Å resolution. *Science*, **246**, 1135–1142.

Schiltz,E. and Rheinbolt,J. (1975) Determination of the complete amino-acid sequence of protein S4 from *Escherichia coli* ribosomes. *Eur. J. Biochem.*, **56**, 467–481.

Siomi,H., Matunis,M.J., Michael,W.M. and Dreyfuss, G. (1993) The pre-mRNA binding K protein contains a novel evolutionarily conserved motif. *Nucleic Acids Res.*, **21**, 1193–1198.

Tanaka,I., Kimura,M., Kimura,J. and Dijk,J. (1984) The amino acid sequence of two small ribosomal proteins from *Bacillus stearothermophilus*. *FEBS Lett.*, **166**, 343–346.

Traut,R.R., Bollen,A., Sun,T.T., Hershey,J.W.B., Sundberg,J. and Pierce,L.R. (1973) Methyl 4-mercaptobutyrimidate as a cleavable cross-linking reagent and its application to the *Escherichia coli* 30S ribosome. *Biochemistry*, **12**, 3266–3273.

Urlaub,H., Kruft,V. and Wittmann-Liebold,B. (1994) New approach for identification of cross-linked peptides to rRNA. *J. Prot. Chem.*, **13**, 480–481.

Vandekerckhove,J., Rombauts,W., Peeters,B. and Wittmann-Liebold,B. (1975) Determination of the complete amino acid sequence of protein S21 from the *Escherichia coli* ribosome. *Hoppe-Seyler's Z. Physiol. Chem.*, **356**, 1955–1976.

Watanabe,K. and Kimura,M. (1985) Location of the binding region for 23S ribosomal RNA on ribosomal protein L2 from *Bacillus stearothermophilus*. *Eur. J. Biochem.*, **153**, 299–304.

Wilson,K.S., Appelt,K., Badger,J., Tanaka,I. and White,S.W. (1986) Crystal structure of a prokaryotic ribosomal protein. *Proc. Natl Acad. Sci. USA*, **83**, 7251–7255.

Wittmann-Liebold,B. and Bosserhoff,A. (1981) Primary structure of protein S2 from the *Escherichia coli* ribosome. *FEBS Lett.*, **129**, 10–16.

Wittmann-Liebold,B. and Marzinzig,E. (1977) Primary structure of protein L28 from the large subunit of *Escherichia coli* ribosomes. *FEBS Lett.*, **81**, 214–217.

Wower,I. and Brimacombe,R. (1983) The localisation of multiple sites on 16S RNA which are cross-linked to proteins S7 and S8 in *Escherichia coli* 30S ribosomal subunits by treatment with 2-iminothiolane. *Nucleic Acids Res.*, **11**, 1419–1437.

Wower,I., Wower,J., Meinke,M. and Brimacombe,R. (1981) The use of 2-iminothiolane as an RNA–protein cross-link agent in *Escherichia coli* ribosomes and the localisation on 23S RNA of the sites cross-linked to proteins L4, L6, L21, L23, L27 and L29. *Nucleic Acids Res.*, **9**, 4285–4302.

Yaguchi,M. (1975) Primary structure of protein S18 from the small *Escherichia coli* ribosomal subunit. *FEBS Lett.*, **59**, 217–220.

Yaguchi,M. and Wittmann-Liebold,B. (1978) The primary structure of protein S17 from the small ribosomal subunit of *Escherichia coli*. *FEBS Lett.*, **87**, 37–40.

Received on May 3, 1995; revised on June 19, 1995